Energetic and Dynamic Aspects of Intramolecular Proton Transfer in 4-Methyl-2,6-diformylphenol: A Detailed Analysis with AM1 Potential Energy Surfaces

S. Mitra, R. Das, S. P. Bhattacharyya,* and S. Mukherjee*

Department of Physical Chemistry, Indian Association for the Cultivation of Science, Jadavpur, Calcutta-700 032, India

Received: May 29, 1996; In Final Form: October 9, 1996[⊗]

The energetics of ground and excited state proton transfer in an isolated 4-methyl-2,6-diformylphenol molecule has been systematically studied by the configuration interaction method at the AM1 level of approximation. The ground singlet and the excited triplet are predicted to have rather large activation barriers on the respective proton transfer paths while the barrier height is much lower on the corresponding singlet surface. The process is predicted to be endothermic in the ground state and exothermic in the excited singlet and more so in the triplet state. From an analysis of the under-barrier vibrational levels supported by the asymmetric double-well potential characterizing two forms, it appears that proton transfer may occur by a vibrationally assisted over-barrier process as well as by a tunneling mechanism following the $S_0 \rightarrow S_1$ excitation. Complex coordinate rotation calculation in the Fourier grid Hamiltonian (FGH) framework shows that the tunneling rate constant from the $\nu = 0$ vibrational level in the S_1 state is of the same order of magnitude as the experimentally obtained rate constant.

Introduction

The study of ultrafast structural changes in electronically excited molecules is an important topic of current research.[1−3] Excited state proton transfer (ESPT) is one of the most simple but important processes in this context. Two types of ESPT reactions have been characterized in the current literature, viz., excited state intramolecular proton transfer ($ESI_{ra}PT$) and excited state intermolecular proton transfer ($ESI_{er}PT$), depending upon the structure of the molecule being studied.[4,5] The former case represents a special class of unimolecular reaction in which the extent of changes in the geometry is very small in the structural isomerization process and is confined to the immediate vicinity of the reaction site within the molecule. In the latter case, electronic excitation of the species causes extensive and rapid charge redistribution within the molecule, making it more acidic in the excited state compared to the ground state. The enhanced acidity in the excited state results in the release of a proton, giving an anion.

ESPT reactions are important in many chemical and biological processes ranging from UV photochemical reactions in plants and mutagenesis to tautomeric interconversion of nucleic acid bases.[6−8] The molecules undergoing ESPT are also important as laser dyes,[9] polymer stabilizers,[10] and switches for pulse shortening of dye laser.[11] Again, as the process is limited to very short time scales, these are of particular interest in the field of fast or ultrafast chemical dynamics.[12,13]

The contemporary literature is replete with studies devoted to the analysis of ESPT processes in heteroatomic compounds from both theoretical and experimental points of view.[14−16] Often, the theoretical results serve as an essential feedback to explain the experimental observations.

Although ab-initio calculations involving extended basis sets with extensive configuration interaction (CI) have been successful in predicting the energetics, structures, and reactivities of small molecules in the ground and excited states, very few reports are available on the ab-initio studies of the excited state proton transfer reactions at the same level of sophistication. This is mainly due to the large size of the molecular systems usually involved and involvement of excited states which are more difficult to handle theoretically.

Scheiner and co-workers studied the proton transfer reactions of intramolecularly hydrogen-bonded compounds using GAUSSIAN 92 and GAMESS programs.[17−19] In a recent study, Luth and Scheiner[20] compared the proton transfer kinetics in isoelectronic compounds like malonaldehyde and 1,5-diaza-1,3-pentadiene. They showed that for both the compounds the PT barrier in the $S_1(\pi\pi^*)$ state is lower than in the S_0 state. A clear relationship between the intramolecular hydrogen bond strength and barrier to the proton transfer was identified. It was also concluded that the higher barrier in 1,5-diaza-1,3-pentadiene, as compared to malonaldehyde, is associated with the weaker hydrogen bond strength in the former. Sobolewski et al.[21,22] studied the potential energy functions of the hydrogen-bonded complex of 2-pyrimidone with water by the ab-initio SCF method using 3-21G and 6-31G** basis sets. They showed that the 2-pyrimidone/water complex is stable in ground state PE surface, and the conversion from the hydroxy form to the oxo form does not occur in this state, even with thermal activation, due to the large barrier height of proton transfer. But in the excited ($\pi\pi^*$) state, the oxo form is more stable, and proton transfer occurs because of 3-fold decrease in the barrier height (from 0.6 to 0.2 eV).

However, semiempirical molecular orbital methods, such as MNDO and AM1, have now become easily accessible utilities in research laboratories. Often, these methods provide good estimates of geometries and heats of formation of organic molecules and insight relating to reaction paths of chemical changes that they undergo.[23] Thus, it is often possible to make predictions about the relative stabilities of similar compounds, construct reaction paths and potential energy surfaces, and predict trends fairly successfully.

Several authors have used the semiempirical calculations within the MNDO,[24] INDO,[25] and AM1[26] levels of approximation to describe ESPT reactions. Catalán et al.[27] carried out semiempirical calculations based on INDO and CNDO/S

* To whom correspondence should be addressed.

[⊗] Abstract published in *Advance ACS Abstracts,* December 1, 1996.

S1089-5639(96)01560-5 CCC: $14.00

methods to describe the efficacy of $ESI_{ra}PT$ as ultraviolet stabilizers in the derivatives of 2-(2′-hydroxyphenyl)benzotriazole (commonly known as Tinuvin P) class of compounds. Calculated results show that the planar structure of Tinuvin P would give two UV transitions at 362 and 306 nm, which exactly reproduces the experimental results. Construction of PE curves along the proton transfer coordinate shows that the proton transferred quinoid form of Tinuvin P is more unstable than the phenolic one in the $1(\pi\pi^*)^1$ state, in contrast with the results obtained for similar compounds 2-(2′-hydroxyphenyl)benzimidazole (HPBI) and 2-(2′-hydroxyphenyl)benzoxazole (HBO).[24] Dick[26] used AM1 and INDO/S calculations to explain the photophysical properties of 3-hydroxyflavone (3HF). It was shown that intramolecular hydrogen bond length data determined from AM1 calculations were fairly close to the X-ray crystallographic results. The relative ordering of the different energy levels corresponding to both normal and tautomeric forms of 3HF in both ground and excited (singlet and triplet) states was determined, and it was shown that in the singlet excited state $n\pi^*$ energy is very close to that of the $\pi\pi^*$ state. Construction of potential energy curves shows although there exists a substantial barrier in the lowest triplet state, proton transfer in the first excited singlet is part of the evolution of a vibrational wave packet on a multidimensional potential energy surface without any barrier on the way to the tautomeric form.[25]

Recently, we have reported some of our experimental work[28,29] on a new proton transfer system, viz., 4-methyl-2,6-diformylphenol (MFOH). The salient features of our findings so far have been (i) in the ground state there exist a strongly hydrogen-bonded keto form, which we call a "closed conformer"; (ii) large Stokes-shifted fluorescence from the electronically excited state is due to the proton transferred "enolic form"; and (iii) the proton transfer reaction in MFOH is relatively slower than in other *o*-hydroxycarbonyl compounds, e.g., *o*-hydroxybenzaldehyde (OHBA) and methyl salicylate (MS), etc.

In the present paper we have conducted a theoretical investigation on the proton transfer reaction of MFOH in a semiempirical framework. We have determined the molecular structures of MFOH in the ground (S_0) and excited (S_1 and T_1) electronic states by use of the AM1 method using configuration interaction where needed. The kinetics and energetics of the proton transfer in each state have been studied at the same level of approximation. The ground (singlet) state calculations have been initially done at the AM1 closed-shell Hartree−Fock (HF) (single determinant) level. The results were then further refined by performing configuration interaction calculations. The CI subspace included the S_0 and $S_1(HOMO^1-LUMO^1)$ + 10 doubly excited (with respect to S_0) configurations. The lowest root corresponds to the ground state while the first excited root refers to the S_1 state. Complete geometry optimization has been carried out at each step while following either the lowest or the first excited root. For the lowest triplet state T_1, initial calculations were performed using the unrestricted Hartree−Fock (UHF) methods at the SCF level. The results were then compared with those of open-shell restricted Hartree−Fock (RHF) calculations. While UHF calculations generally result in somewhat lower energies than corresponding RHF calculations, the former can suffer from spin contamination. It is possible that the contamination of the state of interest by the states of different multiplicities may increase the tendency to break the geometrical symmetry of the molecule while its structure is being optimized. These calculations ultimately lead us to the construction of potential energy surfaces on which the proton transfer is supposed to take place. We then investigated the possible mechanism of proton transfer on these surfaces with special emphasis on the role of tunneling, if any.

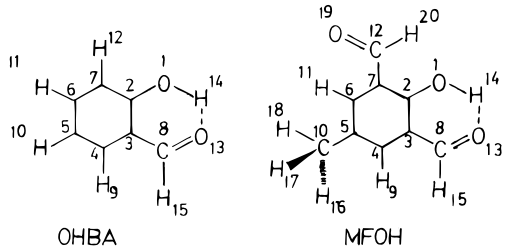

Figure 1. Atom numbering in OHBA and MFOH used for geometry optimization.

TABLE 1: Comparison of AM1 Results of *o*-Hydroxybenzaldehyde (OHBA) with Those of ab-Initio Calculation and Experimental Results[a]

	AM1	ab initio[b]	expt[c]
O1−C2	1.36	1.379	1.36
C2−C3	1.40	1.403	1.39
C3−C8	1.46	1.498	1.46
C8−O13	1.23	1.228	1.22
O1−H14	0.97	0.993	1.04
O13- - -H14	2.02	1.703	
C3−C4	1.40	1.396	1.41
C4−C5	1.38	1.381	
C5−C6	1.40	1.397	1.37
C6−C7	1.38	1.381	1.37
C2−C7	1.41	1.403	1.41
C3−C2−O1	124.9	122.4	
C4−C3−C2	118.4	119.7	
C5−C4−C3	121.1	120.9	
C6−C5−C4	119.9	119.1	
C7−C2−C3	120.4	119.2	
C8−C3−C2	123.4	119.3	
O13−C8−C3	124.3	123.0	
H14−O1−C2	110.1	104.6	

[a] Bond lengths are in angstroms and angles are in degrees. [b] From ref 31. [c] From ref 32.

Results and Discussion

Calibration of the Methodology Used. Since intramolecular hydrogen bonding appears to play an important role in the proton transfer systems under study, we must choose our semiempirical method very carefully. Of the three semiempirical methods available at our disposal, viz., MNDO, MINDO/3, and AM1, AM1 has been known to describe energetics and topographics of H-bonded system fairly accurately.[30] Nevertheless, we have carried out a detailed calculation on a reference molecular system for calibration against available ab-initio results. The reference molecule is *o*-hydroxybenzaldehyde (OHBA, Figure 1). We have optimized the ground state geometrical parameters of OHBA at the AM1 level and compared our results with those obtained by Nagaoka et al.[31] from their ab-initio calculations and Jones et al.[32] from experiments. These results are summarized in Table 1. Our AM1 results show a fair degree of agreement with both the published ab-initio data and results obtained experimentally. We note here that the distance between O13 and H14 atoms is overestimated by about 0.3 Å in the AM1 results relative to available ab-initio data. This discrepancy does not appear to affect the qualitative agreement of the present results with the experimental data. But, it has certainly important bearing on more quantitative information.

Table 2 shows the optimized equilibrium geometrical parameters of MFOH in its two tautomeric forms obtained by the MNDO, MINDO/3, and AM1 methods (see Figure 1 for atom numberings). A close look at the optimized dihedral angle data

TABLE 2: Ground State Geometrical and Energy Parameters of MFOH in Its Two Limiting Stationary Points[a]

	primary			tautomer		
	MNDO	MINDO/3	AM1	MNDO	MINDO/3	AM1
ΔE_t[b]	−2219.99	−2193.47	−2223.39	−2229.46	−2192.79	−2222.85
ΔH_f[c]	−94.87	−103.31	−93.58	−82.57	−87.65	−81.30
O1−C2	1.35	1.31	1.36	1.23	1.21	1.25
C2−C3	1.43	1.43	1.41	1.49	1.51	1.47
C3−C8	1.50	1.49	1.47	1.38	1.38	1.37
C8−O13	1.22	1.19	1.24	1.33	1.29	1.34
O1−H14	0.95	0.95	0.97	2.33	2.49	1.98
O13- - -H14	2.61	2.87	2.00	0.95	0.95	0.98
C3−C4	1.41	1.42	1.40	1.47	1.47	1.44
C4−C5	1.41	1.42	1.39	1.37	1.37	1.36
C5−C6	1.41	1.42	1.40	1.46	1.47	1.44
C6−C7	1.40	1.41	1.39	1.36	1.38	1.36
C2−C7	1.43	1.44	1.42	1.49	1.50	1.47
C3−C2−O1	124.5	125.0	124.4	121.6	120.6	121.3
C4−C3−C2	118.4	115.7	118.9	116.9	116.6	118.8
C5−C4−C3	122.5	125.4	121.5	123.8	125.8	122.1
C6−C5−C4	117.9	114.8	119.0	118.6	115.1	119.4
C7−C2−C3	120.0	123.0	120.1	117.4	118.1	116.7
C8−C3−C2	124.6	125.3	123.3	125.6	126.5	122.2
O13−C8−C3	124.6	128.1	124.3	130.3	134.9	127.7
H14−O1−C2	115.4	117.7	110.3			
H14−O13−C8				117.8	117.6	112.1
H14−O1−C2−C3	7.1	4.0	0.0			
H14−O13−C2−C3				0.4	0.0	0.0
O1−C2−C3−C8	0.3	−2.3	0.0	1.8	0.3	0.0
O13−C8−C3−C2	−55.26	−66.46	0.0	0.2	0.0	0.0

[a] Bond lengths are in angstroms and angles are in degrees. [b] In eV. [c] In kcal mol^{-1}.

clearly indicates nonplanarity of the hydrogen-bonded moiety in MFOH at both MNDO and MINDO/3 levels of approximation. AM1, on the other hand, predicts a planar geometry with considerable hydrogen bonding between the phenolic hydrogen and carbonyl oxygen atoms (O···H distance = 2.00 Å). The deviation from planarity observed in the results obtained by the other two methods of calculation (viz., MNDO and MINDO/3) does not affect the geometrical parameters of the aromatic ring significantly (e.g., the predicted ring bond distances differ by only ±0.01 Å), but the intramolecular hydrogen-bonding parameters are affected considerably (e.g., difference is about ±0.02−0.04 Å). This is also clear from the total energy (ΔE_t) values of the different forms predicted by the different methods of calculation (Table 2). As is well-known, the AM1 method is an improved parametrization for the MNDO Hamiltonian, which has been optimized to reproduce a large set of ground state data of organic molecules.[30] In particular, the description of hydrogen bonding has been claimed to be better in the AM1 method as compared to the original MNDO method. The results pertaining to the ground state of MFOH obtained by the three methods appear to vindicate our choice of the AM1 method for a systematic study of the mechanistic aspects of the proton transfer process in MFOH.

Molecular Structure and Energetics of Proton Transfer in Different Electronic States of MFOH. *S_0 Electronic State.* In the fourth and seventh columns of Table 2, we show AM1 data characterizing proton transfer in MFOH in the S_0 state. The atomic labeling is shown in Figure 1.

The tautomeric form of MFOH resulting from the proton transfer in the ground state is found to be 12 kcal/mol higher in energy than the primary form. It is interesting to note the changes in the bonding pattern observed around the chelate ring (HOCCCO) as the proton is transferred. Comparison of the results given in first and third columns of Table 3 indicates that the "single" bonds have become shorter and the "double" bonds longer in the tautomeric form compared to the primary form. In the benzene ring of the primary form all the C−C bond lengths are predicted to be nearly equal, showing the delocalization of the π orbitals over the entire ring; but, in the tautomeric form, C_4-C_5 and C_6-C_7 bond lengths are predicted to decrease drastically while the others are predicted to increase, signifying that ring current delocalization is partially lost following the proton transfer. The partial loss of aromaticity of the benzene ring following the proton transfer may be the cause of the observed much higher energy of the tautomeric form compared to the primary form. Our result is in conformity with the suggestion of Verner et al.[33], who observed that the keto form of aromatic hydroxy compounds is relatively more stable than the corresponding enolic form.

TABLE 3: Computed Geometrical Parameters of the Transition State Characterizing the Tautomerization of MFOH in the S_0 State[a]

ΔE_t (eV)	−2222.27	C3−C2−O1	119.6
ΔH_f (kcal/mol)	−67.76	C8−C3−C2	116.5
		H14−O1−C2	108.8
O1−C2	1.30		
C2−C3	1.44	H14−O1−C2−C3	0.00
C3−C8	1.41	O1−C2	0.00
C8−O13	1.41	O13−C8	0.00
O1−H14	1.30		
O13−H14	1.18		

[a] Bond lengths are in angstroms and the angles are in degrees; the corresponding parameters for the primary and tautomeric forms are reported in Table 2.

Table 3 reports some of the relevant data for the optimized geometry of the transition state (TS) that characterizes the proton transfer pathway of MFOH in the S_0 state. The optimized bond lengths in the TS structure are intermediate between the two end points. As shown in Table 4, the TS is predicted to be 27 kcal/mol higher in energy than the more stable primary form and structurally planar just as the two tautomeric forms are. The activation barrier is quite high so that proton transfer rate in the S_0 state is expected to be very low, even at room temperature. This corroborates our experimental observation that proton transfer does not take place in the S_0 state of MFOH[28] at all.

TABLE 4: Energetics of Tautomerization of MFOH in S_0, S_1, and T_1 States

	S_0	S_1	T_1
ΔE (kcal/mol) (tautomerization energy)	12.28	−14.38	−13.08 (−8.59)[a]
$\Delta E^{\#}$ (kcal/mol) (activation energy)	25.82	6.39	14.70 (21.46)[a]

[a] Results for UHF calculations.

TABLE 5: Computed Geometrical Parameters of all the Stationary Points Characterizing the Tautomerization of MFOH in the S_1 State[a]

	closed	TS[b]	tautomer
ΔE_t (eV)	−2219.45	−2219.17	−2220.07
ΔH_f (kcal/mol)	−2.84	3.55	−17.22
O1−C2	1.33	1.29	1.25
C2−C3	1.44	1.47	1.47
C3−C8	1.44	1.43	1.43
C8−O13	1.26	1.31	1.33
O1−H14	0.987	1.17	1.93
O13- - -H14	1.89	1.21	0.98
C3−C2−O1	123.4	118.7	120.7
C8−C3−C2	121.4	114.8	120.5
H14−O1−C2	112.6	110.2	
H14−O13−C8			112.9
H14−O1−C2−C3	−0.16	0.08	
H14−O13−C8−C3			0.15
O1−C2−C3−C8	0.04	0.24	0.72
O13−C8−C3−C2	0.11	−0.33	−1.47

[a] Bond lengths are in angstroms and the angles are in degrees. [b] Transition state.

S_1 Electronic State. Table 5 shows the *12-configuration* CI optimized geometry of all the relevant stationary points along with their energetics during the proton transfer in the S_1 electronic state of MFOH. Most interestingly, the tautomeric (enolic) form in this state is predicted to be more stable than the primary form by about 14.4 kcal/mol. Thus, the endothermic proton transfer process in the ground state of MFOH is predicted to become an exothermic one in the S_1 state.

Comparing the computed geometrical parameters of MFOH in the S_0 (primary) and S_1 (tautomer) states, one can see that drastic changes have occurred in the hydrogen-bonded chelate ring. The O1−C2 single bond in the primary form has been converted into a double bond similar to the C3−C8 bond, and the C8−O13 double bond of the carbonyl moiety has been converted into a single bond. On the whole, the phenolic structure in the ground state is predicted to have been converted into an enol-like structure upon $S_1 \leftarrow S_0$ excitation, which is consistent with our experimental results.[28,29]

The observed changes in the energetics and topography accompanying $S_1 \leftarrow S_0$ excitation can be qualitatively understood from the nature of the frontier orbitals of the two tautomeric forms (Figure 2) in the S_0 states. The HOMO of the primary form is more stable by about 0.5 eV than that of the tautomer in the S_0 state. This may be because the former corresponds mainly to the symmetric contributions from the 2p π atomic orbitals of C2, C3, C7 and C4, C5, C6, whereas in the latter (tautomer) case the bonding contributions are only from C3, C4, C5 2p π atomic orbitals. On the other hand, the LUMO of the tautomeric form has more bonding contribution than that of the primary form, and the balance is such that it is stabilized by about 0.5 eV over the LUMO of primary (closed) form of MFOH. The HOMO−LUMO energy difference is therefore less in the tautomeric form than in the primary (closed) form. If one neglects electron repulsions, this would tend to suggest that the tautomeric form gets stabilized upon $S_1 \leftarrow S_0$ excitation. Moreover, the participation of the carbonyl oxygen is very small in the HOMO, but the reverse is true for its participation in the LUMO; i.e., HOMO → LUMO excitation allows electron density to flow to the carbonyl oxygen. From a conventional chemical point of view, the carbonyl oxygen therefore becomes more electron rich (basic) and the phenolic group becomes more acidic on excitation, thereby facilitating proton transfer.

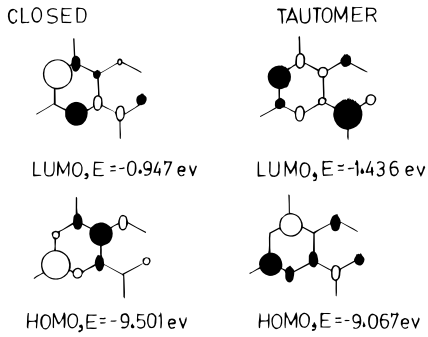

Figure 2. Composition of the frontier orbitals of two stationary points of MFOH.

TABLE 6: Computed Geometrical Parameters of All the Stationary Points Characterizing the Tautomerization of MFOH in the T_1 State[a]

	closed	TS[b]	tautomer
ΔE_t (eV)	−2220.90	−2220.24	−2221.46
ΔH_f (kcal/mol)	−35.75	−21.05	−48.83
O1−C2	1.35	1.33	1.25
C2−C3	1.48	1.48	1.48
C3−C8	1.45	1.44	1.41
C8−O13	1.24	1.25	1.34
O1−H14	0.976	1.20	1.99
O13- - -H14	1.99	1.78	0.973
C3−C2−O1	123.0	122.6	121.6
C8−C3−C2	122.6	122.8	121.6
H14−O1−C2	110.8	110.3	
H14−O13−C8			111.4
H14−O1−C2−C3	3.72	−7.82	
H14−O13−C8−C3			0.02
O1−C2−C3−C8	−3.50	−9.98	−0.70
O13−C8−C3−C2	8.28	2.10	−0.00

[a] Bond lengths are in angstroms and the angles are in degrees. [b] Transition state.

T_1 Electronic State. The fully optimized topographic and energy parameters of all the stationary points of MFOH in the T_1 state, calculated with the open-shell restricted Hartree−Fock (RHF) method followed by three-configuration CI, are given in Table 6. A close look into the values displayed shows that the predicted changes in geometrical parameters in the T_1 state parallel what has been observed in the S_1 state. From Table 6, it is seen that the tautomeric form is stabilized by about 13.1 kcal/mol more than the closed form in the triplet. Hence, there is a possibility for the proton transfer to be thermodynamically feasible in the T_1 electronic state also, provided the activation barrier for the process is low enough. But from Table 4 we can see that the activation barrier to the proton transfer in the T_1 state is quite high. It is therefore unlikely that any significant degree of proton transfer occurs in the excited triplet under ordinary conditions by the over-barrier process. Although calculations with the unrestricted Hartree−Fock (UHF) method stabilize the energy parameters of all the three points to some extent (Table 4), this method was discarded due to the possibility of spin contamination. But it is to be mentioned here that qualitative kinetic description of proton transfer of MFOH in

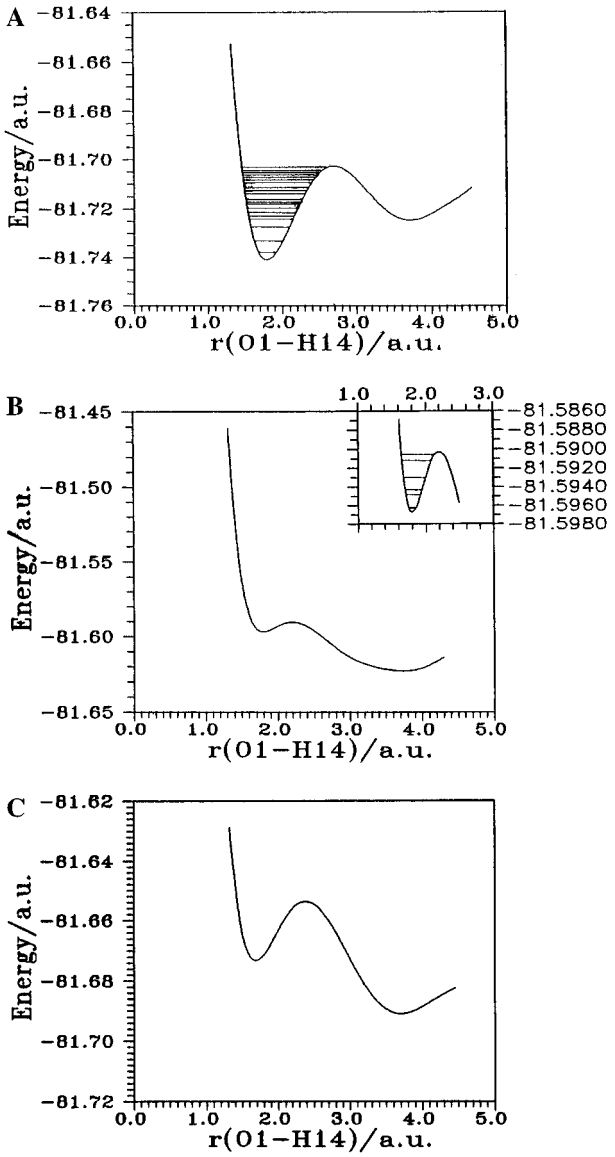

Figure 3. (A) Variation of total energy during the proton transfer in the S_0 state. The horizontal lines indicate the position of vibrational levels up to the barrier in the primary well calculated by the Fourier grid Hamiltonian (FGH) method. (B) Variation of total energy during the proton transfer in the S_1 state. The horizontal lines indicate the position of vibrational levels up to the barrier in the primary well calculated by the FGH method. (C) Variation of total energy during proton transfer in the T_1 state.

this state remains same *whether an unrestricted HF or a restricted HF method is used* in the present problem.

Proton Transfer Mechanism and the Reaction Path Analysis. To construct the reaction path representing the proton transfer in MFOH, the O1−H14 distance (r) was chosen as the coordinate. As the proton translocation distance of the mobile hydrogen atom is considered to be a key parameter for the construction of the $ESI_{ra}PT$ potential,[24] the O1−H14 distance was varied between what is normal for the primary and what is known to be the equilibrium tautomeric O1−H14 distance. At each such point, all other geometrical parameters were fully optimized (with 12-configuration CI in S_0 and S_1 states), and the total energy (ΔE_t) was plotted against r. Interpolation through cubic spline was used to construct the potential energy (PE) curves representing the proton transfer process. Parts A, B, and C of Figure 3 show the PE curves for the S_0, S_1, and T_1 states of MFOH, respectively. All the figures show two distinct minima corresponding to the primary and tautomeric forms. In each case the curve passes through a maximum which is the saddle point (SP) on the proton transfer path as confirmed by the diagonalization of the relevant force constant matrix at the particular point.

The asymmetric double-well potentials as obtained here for the S_0 and S_1 states may appear to be inconsistent with our previous experimental observations at the first sight. This is because we have reported earlier that in nonpolar solvents MFOH exists only in "closed form" in the S_0 state while in the S_1 state only the proton transferred or "tautomeric" form exists. But our calculations on MFOH can be assumed to represent an extreme case of "reverse asymmetry" in the S_0 and S_1 states which is very common to intramolecularly hydrogen-bonded *o*-hydroxy compounds.[34]

The maximum in the S_0 state is a true saddle point on the potential energy surface (PES) and occurs at a proton transfer distance of 1.30 Å. Table 4 shows the exo(endo)thermicities and activation energies for the tautomerization process of MFOH in each of the three states. It turns out that the reaction is appreciably endothermic in the S_0 state. The activation energy ($\Delta E^{\#}$) for the proton transfer is also rather high. So, proton transfer in this state is quite unlikely. On the other hand, the proton transfer reaction is predicted to be exothermic in both the S_1 and T_1 states. But, considering the activation energies for proton transfer in these states, it can be said that in spite of tautomerization being thermodynamically favored in the T_1 state, kinetic constraints (high $\Delta E^{\#}$) can inhibit the process on the triplet PES. Again, a very small proton transfer barrier in the S_1 state (as compared to the appreciably high value in the S_0 or T_1 states) is indicative of a rather shallow well characterizing the primary form. It may not be deep enough to contain an appreciable number of bound vibrational levels, so that the potential is effectively of the anharmonic single well type for all intents and purposes.

The fact that we have observed experimentally only the tautomeric emission from the S_1 state can now be explained in light of the nature of PES obtained theoretically, which points to a strongly asymmetric double-well potential in which the proton moves. Since Franck−Condon excitation from the S_0 state could result in vibrational excitation on the S_1 surface, we would like to explore whether such an excitation would effectively reduce the barrier height operative in the proton transfer process on the excited (S_1) surface further. We have obtained fairly accurate estimates of vibrational levels and the corresponding eigenfunctions supported by the S_0 and S_1 surfaces using the Fourier grid Hamiltonian (FGH) recipe.[35] In the Figure 3A,B the primary well on the S_0 surface supports approximately 20 vibrational levels under the barrier while the S_1 surface accommodates only six vibrational levels under the barrier separating the primary well from the tautomeric well. From the nature of the S_0 and the S_1 surfaces (Figure 3A,B) it appears that in the FC excited S_1 state the vibrational excitation would take the system almost over the barrier and eventually into the potential well representing the tautomeric form. It would then explain why we have observed only the tautomer emission from the S_1 state. It need not necessarily mean that S_1 surface has a single potential well. We may conclude therefore that the proton transfer process on the S_1 state *may well be a vibrationally assisted over-barrier process at room temperature*. It is difficult to estimate at this stage whether, and if at all, tunneling contributes to the proton transfer rate. In order to assess the possibility of any significant degree of proton transfer from the primary to the tautomer well occurring by tunneling, we have carried out FGH-based complex coordinate rotation calculations[36] of the lifetimes of the vibrational levels

supported by the S_0 and S_1 surfaces. The inverse of the lifetime gives the tunneling rate. It appears that tunneling of the proton from the lowest vibrational levels ($\nu = 0$, 1, ... etc.) in the S_0 state is very slow while the situation is quite different in the S_1 state ($\sim 10^{11}$ s^{-1}). Here, the predicted tunneling rate constant from the ground or first excited vibrational level is of the same order of magnitude as observed experimentally. (The experimental rate is an average over the accessible vibrational levels.) It is therefore very difficult to negate the tunneling mechanism for the proton transfer in the S_1 state of MFOH on the basis of our theoretical calculations. Experiments at 4 K and more refined theoretical calculations are needed to settle this point unambiguously.

For methyl salicylate (MS), a compound structurally similar to MFOH, Smith and Kaufmann[37] proposed a zwitterionic structure as the fluorescing state. In our experiment, we have previously shown that MFOH fluorescence does not correlate with the solvent dielectric properties,[38] negating the possible existence of zwitterionic structure. Again, computed electron densities on the O1 and O13 atoms in the S_1 state are quite close to each other (8.20 and 8.35, respectively). Therefore, the fluorescing state of MFOH can be regarded as far less ionic. In fact, the transfer process appears to be more like a "hydrogen" transfer process rather than a purely proton transfer process.

Conclusions

The AM1 calculations on the S_0, S_1, and T_1 states of MFOH tend to suggest the following scenario for the thermodynamics and the kinetics of proton transfer process.

(i) The process is thermodynamically endothermic in the ground state and also encounters high activation barrier.

(ii) In the S_1 and T_1 states, however, the process becomes naturally exothermic. But, the barrier turns out to be rather high on the triplet surface.

(iii) FC excitation from the S_0 to the S_1 state of the primary form takes the molecule to a point on the S_1 surface where the over-barrier transfer of the proton becomes facile. MFOH is therefore likely to emit only from the tautomeric form even in nonpolar solvents.

(iv) Complex scaled FGH calculation shows that in ESPT process of MFOH tunneling mechanism can coexist with over-barrier mechanism. Only very low-temperature studies and refined theoretical calculations of the dynamics can finally settle this point.

Acknowledgment. The authors thank Mr. P. Sarkar of this department for his help in doing the Fourier grid analysis. S. Mitra and R. Das are the recipients of a fellowship from University Grants Commission and Council of Scientific and Industrial Research, respectively. All the calculations were carried out in a DEC 2000 αXP computer procured under a research grant from Department of Science and Technology, Government of India.

References and Notes

(1) Choi, K.-J.; Boczer, B. P.; Topp, M. R. In *Ultrafast Phenomena IV*; Auston, D. H., Eisenthal, K. B., Eds.; Springer: New York, 1984; p 368.
(2) Laermer, F.; Elsaesser, T.; Kaiser, W. *Chem. Phys. Lett*. **1988**, *148*, 119.
(3) Special issue on "Photon-induced molecular dynamics": Aquilanti, V.; Guidoni, A. G.; Lee, Y. T. *Chem. Phys*. **1994**, *187*.
(4) Aranut, G. L.; Formosinho, J. S. *J. Photochem. Photobiol. A: Chem*. **1993**, *75*, 1.
(5) Koswer, E. M.; Huppert, D. *Annu. Rev. Phys. Chem*. **1986**, *37*, 127.
(6) Kwiatkowski, J. S.; Zielinski, T. J.; Rein, R. *Adv. Quantum Chem*. **1986**, *18*, 85.
(7) Kooper, W. G. *Int. J. Quantum Chem*. **1978**, *14*, 71.
(8) Topal, M. D.; Fresco, J. R. *Nature* **1976**, *263*, 285.
(9) Nagaoka, S.; Fujita, M.; Takemura, T.; Baba, H. *Chem. Phys. Lett*. **1986**, *123*, 489.
(10) Werner, T.; Woessner, G.; Kramer, A. E. H. In *Photodegradation and Photostabilization of Coatings*; Pappas, S. P., Winslow, F. H., Eds.; ACS Symposium Series 151; American Chemical Society: Washington, DC, 1981; p 1.
(11) Ernsting, N. P.; Nikolaus, B. *Appl.Phys. B* **1986**, *39*, 155.
(12) Bogris, D. In *Electron and Proton Transfer in Chemistry and Biology*; MÅller, A., Ratajczak, H., Junge, W., Diemann, E., Eds.; Elsevier: Amsterdam, 1992; p 345.
(13) Barbara, P. F.; Walker, C. G.; Smith, T. P. *Science* **1992**, *256*, 975.
(14) Special issue on Proton Transfer: Barbara, P. F., Tommsdorf, H. P., Eds. *Chem. Phys*. **1989**, *136*, 153−360.
(15) Wortmann, R.; Elich, K.; Lebus, S.; Liptay, Y.; Borowicz.P.; Graboska, A. *J. Phys. Chem*. **1992**, *96*, 9724.
(16) Schiener, S. *Acc. Chem. Res*. **1994**, *27*, 402.
(17) Schiener, S. *Acc. Chem. Res*. **1985**, *18*, 174.
(18) Schiener, S. In *Proton Transfer in Hydrogen Bonded Systems*; Bountis, T., Ed.; Plenum; New York, 1992; p 29.
(19) Luth, K; Scheiner, S. *J. Phys. Chem*. **1994**, *98*, 3582.
(20) Luth, K; Scheiner, S. *J. Phys. Chem*. **1995**, *99*, 9854.
(21) Sobolewski, A. L.; Domcke, W. *Chem. Phys. Lett*. **1993**, *211*, 82.
(22) Sobolewski, A. L.; Adamowicz, L. *J. Phys. Chem*. **1995**, *99*, 14277.
(23) Belletàte, M; Leclerc, M.; Durocher, D. *J. Phys. Chem*. **1994**, *98*, 9450.
(24) Engeland, T. A.; Bultmann, T.; Ersting, N. P.; Rodriguez, M. A.; Theil, W. *Chem. Phys*. **1992**, *163*, 43.
(25) MÅhlpfordt, A.; Bultmann, T.; Ernsting, N. P.; Dick, B. *Chem. Phys*. **1994**, *181*, 447.
(26) Dick, B. *J. Phys. Chem*. **1990**, *94*, 5752.
(27) Catalán, J.; Faberio, F.; Guijarro, M. S.; Claramunt, R. M.; Santa Mar×c1a, M. D.; Foces-Foces, M. C.; Cano, F. H.; Elguero, J.; Sastre, R. *J. Am. Chem. Soc*. **1990**, *112*, 747.
(28) Mitra, S.; Das, R.; Mukherjee, S. *Chem. Phys. Lett*. **1993**, *202*, 549.
(29) Das, R.; Mitra, S.; Mukherjee, S. *Chem. Phys. Lett*. **1994**, *221*, 368.
(30) Dewar, M. J. S.; Zoebisch, E. G.; Healy, E. F.; Stewart, J. J. P. *J. Am. Chem. Soc*. **1985**, *107*, 3902.
(31) Nagaoka, S.; Nagashima, U. *Chem. Phys*. **1989**, *136*, 153.
(32) Jones, H.; Curl Jr., R. F. *J. Mol. Spectrosc*. **1972**, *42*, 65.
(33) Verner, M. V.; Schiener, S. *J. Phys. Chem*. **1995**, *99*, 642.
(34) Formosinho, J. S.; Aranut, G. L. *J. Photochem. Photobiol. A: Chem*. **1993**, *75*, 21.
(35) Marston, C. C.; Balint-Kurty, G. G. *J. Chem. Phys*. **1989**, *91*, 3571; Dutta, P.; Adhikari, S.; Bhattacharyya, S. P. *Chem. Phys. Lett*. **1993**, *212*, 677.
(36) Adhikari, S; Dutta, P, Bhattacharyya, S. P. *Chem. Phys. Lett*. **1996**, *248*, 218. Chu, S. I. *Chem. Phys. Lett*. **1990**, *167*, 155.
(37) Smith, K. K.; Kaufmann, K. J. *J. Phys. Chem*. **1981**, *85*, 2895.
(38) Mitra, S.; Das, R.;Mukherjee, S. *Spectrochim. Acta, Part A* **1994**, *50*, 1301.